alloys

MDPI

Article

Research on the Corrosion Resistance and Cytotoxicity of Medical Forged Co-28Cr-6Mo Alloy

Bo Xu [1,2], Yangtao Xu [1,2,3,*] and Jianglong Wei [1,2]

[1] State Key Laboratory of Advanced Processing and Recycling of Nonferrous Metals, Lanzhou University of Technology, Lanzhou 730050, China; 193129155672@163.com (B.X.); 13364310690@163.com (J.W.)
[2] School of Materials Science and Engineering, Lanzhou University of Technology, Lanzhou 730050, China
[3] Gansu Natural Energy Research Institute, Lanzhou 730030, China
* Correspondence: xuyt@lut.edu.cn; Tel.: +86-13893236182

Abstract: Co-Cr-Mo alloy as a human body implant material has a long history, because of its excellent corrosion resistance and biocompatibility, and is widely used in human hip joint materials. Co-Cr-Mo alloy in the human body is often in a passivation state; the formation of dense oxide film on the alloy surface prevents further corrosion of the alloy. The main component of the passivation film is the oxide of Cr, so a layer of oxide film formed by Cr on the surface of Co-Cr-Mo alloy is the reason for its good corrosion resistance. In biocompatibility, cytotoxicity is the first choice and necessary option for biological evaluation, and cytotoxicity can quickly detect the effect of materials on cells in a relatively short time. Therefore, this research conducted a comparative evaluation on the corrosion resistance and biocompatibility of forged Co-Cr-Mo alloys produced in domestic and foreign alloys in line with medical standards. Three simulated human body fluids and Princeton electrochemical station were selected for corrosion resistance experiments, and it was found that the corrosion resistance of four alloys in sodium citrate solution inside and outside China would be reduced. All the alloys exhibit secondary passivation behavior in Hanks solution, which improves the corrosion resistance of the alloys. According to the self-corrosion potential Ecorr analysis, the corrosion resistance of domestic B alloy is the best, while that of foreign R31537 alloy is poor. In the biocompatibility experiment, the biocompatibility of Co-Cr-Mo alloy was evaluated through the measurement of contact Angle and cytotoxicity reaction. The experimental results show that Co-Cr-Mo alloy is a hydrophilic material, and the contact Angle of foreign R31537 alloy is smaller, indicating that the surface of R31537 alloy is more suitable for cell adhesion and spreading. According to the qualitative and quantitative analysis of the cytotoxicity experiment, the toxic reaction grade of domestic A, B and R31537 alloy is grade 1, the toxic reaction grade of C alloy is grade 2, and C alloy has a slight toxic reaction.

Keywords: Co-Cr-Mo alloy for medical purposes; corrosion resistance; biocompatibility; cytotoxicity

Citation: Xu, B.; Xu, Y.; Wei, J. Research on the Corrosion Resistance and Cytotoxicity of Medical Forged Co-28Cr-6Mo Alloy. *Alloys* **2024**, *3*, 269–280. https://doi.org/10.3390/alloys3040016

Academic Editors: Frank Czerwinski and Nikki Stanford

Received: 14 August 2024
Revised: 14 October 2024
Accepted: 15 October 2024
Published: 18 October 2024

1. Introduction

Biological metal materials are metal or alloy as a kind of inert material for medical devices. Compared with other biological materials, biological metal materials have good mechanical properties and fatigue resistance, and the processing process is simple, which makes biological metal materials widely considered in clinical medicine. It can repair the damaged cardiovascular and soft tissues or replace the hard tissues [1] such as human joints. Commonly used biological metal materials are mainly medical stainless steel [2], titanium alloy [3] and cobalt alloy [4]; medical cobalt-based alloy is divided into casting and forging Co-Cr-Mo alloy. Co-Cr-Mo alloy as a human body implant material has a long history; 1929 casting Co-Cr-Mo alloy began to be applied in the dental field; in the 1950s, Co-Cr-Mo alloy was successfully applied to clinical orthopedics, with good application for artificial hip and knee replacement [5]. At that time, the Co-Cr-Mo alloy was basically

cast Co-Cr-Mo alloy, whereby in the casting process, there were coarse grains and pores, inclusions and other defects, so that the strength and ductility of casting Co-Cr-Mo alloy was poor, and the forged Co-Cr-Mo alloy began to enter people's vision. Forged Co-Cr-Mo alloy made up for some defects of cast Co-Cr-Mo alloy, which improved in strength and ductility, and began to be gradually used in the manufacture of artificial joints. Co-Cr-Mo alloy has a low coefficient of thermal expansion and high thermal conductivity, and the elastic modulus does not change with the increase in its strength, because of its high fatigue resistance and excellent strength and is used for the human body which bears larger hip and knee [6–8] joints.

Co-Cr-Mo alloy also has good corrosion resistance, often in the human body when in a passivation state. The passivation of the metal means that in a given environment, although the metal has obvious thermodynamic possibilities, it still shows a large corrosion resistance, which is due to the dense oxide film formed on the alloy surface to prevent further corrosion [9] of the alloy. Passivation film is when the alloy is under certain conditions, the components in the physiological environment are directly combined with the metal surface atoms, or combined with dissolved metal ions and generated. Passivation film is generally very thin, and the dissolution rate is very low; dissolution occurs in the membrane/solution interface of the electrochemical process, and the dissolution rate and membrane/solution interface of the double layer potential difference are related [10,11]. Co-Cr-Mo alloy has good corrosion resistance due to its spontaneous formation of passivation film; the formation of passivation film will reduce the release of metal ions, and passivation film on Co-Cr-Mo alloy corrosion resistance plays an important role. In the physiological environment, passivation film will change with time. Some passivation film damage is due to pitting caused by gap corrosion or wear corrosion. It is also possible that the ions in the electrolyte are adsorbed to the passivation film and react with the metal or promote the selective dissolution of the passivation film of a specific component. Co-Cr-Mo alloy passivation film is the main component of Cr oxides, a small part of Mo and Co oxides, so Cr in the Co-Cr-Mo alloy surface forming a layer of oxide film is the reason for its good corrosion resistance, and the alloy Mo can improve the corrosion resistance [12] of the alloy in Cl^- solution.

As one of the most common biological metal materials, Co-Cr-Mo alloy also has good biocompatibility. Emma Louise M et al. found that Ni ion was the main factor leading to a cytotoxic reaction by comparing the cell morphology co-culture of Co-Cr alloy and Ni-Cr alloy with oral keratinocytes and detecting cell density and gene expression of inflammatory cells. The dissolution of Ni ion led to the expression of inflammatory genes IL-8, IL-1a and PGE2. The Co-Cr alloy showed no cytotoxic reaction and no expression of inflammatory genes, which showed good biocompatibility. Non-toxicity is the first principle of biocompatibility evaluation; in biocompatibility, cytotoxicity is the first choice for biological evaluation and a necessary option; cytotoxicity can quickly detect the impact of materials on cells in a relatively short period of time, so the experiment on the cytotoxicity of implant materials is particularly important in the evaluation [13–15] process of Co-Cr-Mo alloy biocompatibility.

In this paper, the forged Co-Cr-Mo alloy developed by three domestic professional enterprises producing medical alloys and the products developed by the American Carpenter company were studied, comparing the differences in corrosion resistance and biocompatibility of the forged Co-Cr-Mo alloy for medical purposes, and analyzing the reasons for the differences.

2. Experimental Materials and Methods

2.1. Experimental Materials

In this research, three kinds of alloys, A, B and C, produced by three domestic enterprises and R31537 alloy produced by Carpenter Technology in the United States were tested. The dual process of vacuum induction melting furnace and electroslag remelting furnace was used to prepare the alloy. After forging and rolling, the electroslag ingot

was sampled and tested, and the chemical composition was obtained in Table 1. For the content control of impurity elements Si, Mn, etc., the process was carried out according to ASTM F1537 and ISO 5832-12 mentioned in the standard; the Si and Mn element mass percentage (wt%) was in the range of 0–0.1 for qualified products. Figure 1 shows the metallographic micrograph of Co-Cr-Mo alloy. The alloy plates in domestic and foreign were processed into 10mm×10mm×10mm blocks by wire-cutting technology. After polishing with sandpaper of different particle sizes, electrolytic polishing was carried out, and the electrolyte was 1:9 H_2SO_4:CH_3OH solution with voltage 13V and current 1.5A. The polishing time was 30s, and the etching solution of HCl:H_2SO_4:HNO_3 with the volume ratio of 95:3:2 was configured. The electrolytically polished sample was immersed in the etching solution for about 30s, cleaned with anhydrous ethanol, and observed under an optical microscope. Table 2 shows the mechanical properties of Co-Cr-Mo alloy.

Table 1. Chemical composition of four alloys examined in this research (wt%).

	Co	Cr	Mo	C	Ni	Fe	N	Impurity
A alloy	64.73	27.85	6.05	0.11	0.20	0.28	–	0.78
B alloy	63.30	28.22	6.00	0.20	0.80	0.30	–	1.18
C alloy	64.24	27.44	6.30	0.18	0.65	0.49	–	0.67
R31537 alloy	66.418	26.50	6.02	0.096	0.20	0.44	0.18	0.15

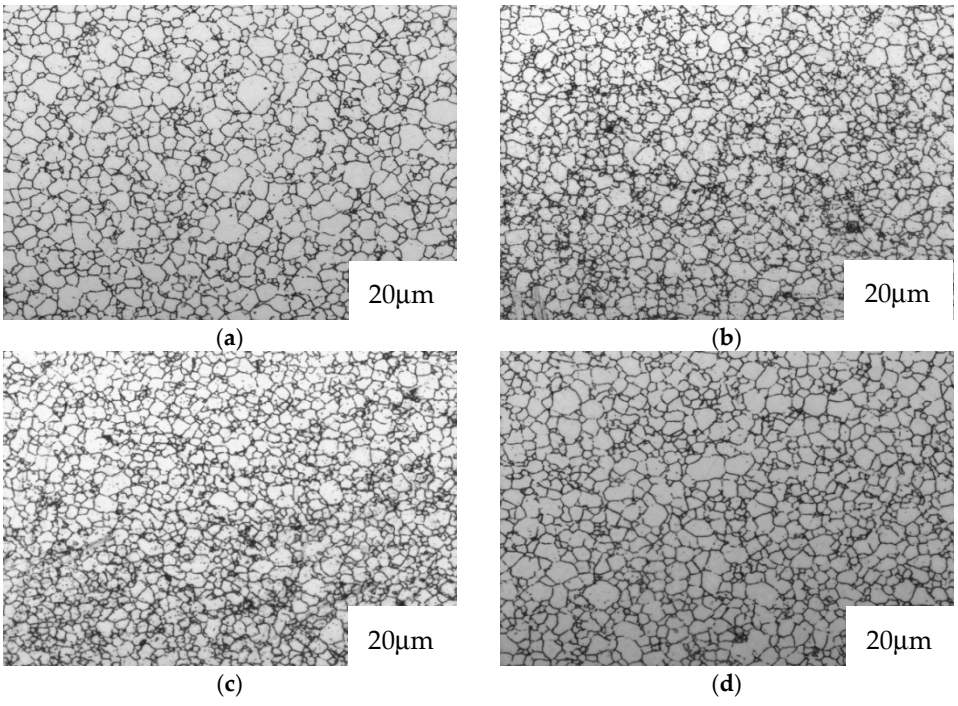

Figure 1. Optical micrographs of (**a**) alloy A; (**b**) alloy B; (**c**) alloy C; (**d**) R31537 alloy.

Table 2. Mechanical properties of alloys examined in this research.

	Tensile Strength (MPa)	Yield Strength (0.2%) (MPa)	Elongation After Breaking (%)	Reduction in Area (%)	Hardness (HRC)
A alloy	1184	874	14.79	14.43	39.9
B alloy	1195	876	14.80	14.55	39.8
C alloy	1153	865	14.82	14.32	39.3
R31537 alloy	1082	794	19.68	18.94	40.3
Standard	1000	700	12	12	28

2.2. Experimental Methods

2.2.1. Corrosion Resistance Test

The Co-Cr-Mo alloy produced in domestic and foreign alloys was processed into square blocks of 8 × 8 × 8 mm and square sheets of 10 × 10 × 2 mm by wire cutting technology, and the corrosion resistance and biocompatibility of Co-Cr-Mo alloy were studied. Different parts of the human body correspond to different pH values; the research found that the pH value of the human hip joint is about 7, so the Co-Cr-Mo alloy corrosion resistance experiment selected a 0.9%NaCl solution, sodium citrate solution and Hanks' solution as the medium, because the pH of these three solutions is about 7 and very similar to the environment of human body fluids. The corrosion resistance of each element in the alloy is different, and the effect in the solution is also different. After grinding the domestic and foreign samples with sandpaper, mechanical polishing and cleaning the surface with alcohol and drying, the remaining surface of the sample except the surface to be tested was sealed, and the potential current density anode polarization curve was determined by Princeton electrochemical station. The experimental process was kept in a constant temperature water bath of 36.5 °C. The working electrode experiment sample, reference electrode saturated calomel electrode and auxiliary electrode platinum electrode were used. The alloy was put into the solution for 1 h, and the scanning began after it was stabilized, and the scanning rate was 40 mV/min.

2.2.2. Cytotoxicity Test

The biocompatibility experiment was mainly to detect the cell hydrophilicity and cytotoxicity of Co-Cr-Mo alloy. In the hydrophilic experiment, the contact Angle of the surface of four kinds of alloys was analyzed by the contact Angle instrument. In the experiment, the LSA 100 optical contact Angle tension tester was selected, and the 2.5 μL deionized water droplets were deposited on the surface of the alloy by the hanging drop method. The contact Angle of the alloy surface was calculated by the three-point fitting method. The hydrophilicity of the surface of the alloy was analyzed.

Mouse osteoblasts were selected for cytotoxicity testing, and the experiment was divided into blank control group (control), A, B, C and R31537 (Sample). After sterilization, the samples were soaked twice with sterile PBS on the surface, and three samples in each group of four groups were placed in three 12-well plates. MC3T3-E1 cell suspension with a logarithmic growth stage was adaptively cultured in a complete medium (89%MEM + 10%FBS + 1%P/S) for 2 generations, and the cell density was adjusted to 5×10^4 cells/mL according to the counting results. The suspensions were inoculated into three 12-well plates with a 1 mL medium per well, and divided into five groups. The cell-free complete medium holes were also designated as blank holes. The remaining holes were added with sterile PBS buffer and continued to be cultured for 24 h. After the end of incubation, the original medium was removed and 1 mL of CCK8 working solution (90%MEM + 10%CCK8 test solution) was added. The holes without cells were used as blank holes, and after proper incubation time, 100 μL of the incubated working solution was sucked out of each hole. The light absorption value at 450 nm was measured on the enzyme-labeled instrument. The cell survival rate of each group and the differences between groups were calculated. The calculation formula was

$$\text{Cell Viability}(\%) = 100\% \times (\text{OD}_{\text{Sample}} - \text{OD}_{\text{Blank}})/(\text{OD}_{\text{Control}} - \text{OD}_{\text{Blank}}) \quad (1)$$

The cytotoxicity of the sample for testing could be determined on the basis of cell state observation and cell viability test results. The evaluation methods were divided into qualitative evaluation and quantitative evaluation, as shown in Tables 3 and 4. The evaluation criteria were as follows: when the reaction grade was 0–1, the experimental results were qualified; when the reaction grade was level 2, it combined with the comprehensive analysis of cell morphology; when the reaction grade was 3–5, the experimental results were not qualified [16].

Table 3. Qualitative classification of cytotoxic reactions.

Levels	Level of Reaction	Cell Watch
0	None	No reaction area observed around and under the specimen
1	Slight	There is a portion of malformed and degenerated cells below the specimen
2	Light	The reaction area is limited to the area below the specimen
3	Medium	The reaction area exceeds the sample size to 1 cm
4	Heavy	The reaction area exceeds the sample size to more than 1 cm

Table 4. Quantitative classification of cytotoxic reactions.

Levels	0	1	2	3	4	5
Cell proliferation rate	≥100	75–99	50–74	25–49	1–24	0

3. Experimental Results and Analysis

3.1. Analysis of Corrosion Resistance of Co-Cr-Mo Alloy in Domestic and Foreign Alloys

The typical anode polarization curve of Co-Cr-Mo alloy can be divided into three stages. First, the region where the current increases with the increase in potential is called the activation region. Secondly, with the increase in potential, the current almost remains unchanged, which is the passivation zone. Finally, the current increases again with the increase in potential, which is the transpassivation area. Because the metal potential in different electrode reactions is in different sections, the corrosion rate of metal is different; if the potential is maintained in the passivation zone [17], the corrosion rate is at a minimum. Whether the corrosion potential of metal can be in the passivation zone is not only related to the size of the passivation zone in the anode polarization curve, but also related to the position of the anode polarization curve [18,19]. The results of anode polarization curves of four kinds of alloys in Figure 2 show that the initial stage of anode polarization with a potential less than 0.5 V is a natural passivation zone, and the current density changes little with the increase in potential in this process. The alloy is protected by a dense passivation film on the surface and is not easy to corrode. The main components of the passivation film are oxides and hydroxides of Cr^{3+}. When the potential reaches about 0.5 V, the current rises sharply, at this time Cr^{6+} is further oxidized to Cr^{3+}, the passivation film begins to dissolve, and the alloy corrosion intensifies; this stage is called the over-passivation stage. After the alloy potential reaches about 0.8 V, the alloy surface will occur at the H_2O oxidation stage, and this stage polarization curve slope is $small_2$, where corrosion tends to be stable.

According to the anode polarization curves of the samples in the three groups of solutions, it can be found that the polarization curves in NaCl solution and 0.05 M/L sodium citrate solution are typical anode polarization curves of Co-Cr-Mo alloys, while before the H_2O oxidation stage in Hanks solution, all the four alloys have a secondary passivation behavior, at which time the current is stable. The corrosion rate of the alloy is stable, which means that the Co-Cr-Mo alloy is protected by the passivation film again, resulting in slow corrosion. The reason for this phenomenon is that some inorganic ions in the Hanks solution, such as $H_xPO_4^{n+}$, SO_4^{2-} and glucose, transform Cr^{3+} into Cr^{6+} oxide, resulting in secondary passivation of the alloy. The existence of the secondary passivation stage improves the corrosion resistance of the alloy. This indicates that the presence of various ions in Hanks solution has a certain effect on the corrosion resistance of Co-Cr-Mo alloy.

In Figure 2, the transpassivation potential of the four gold combinations in 0.9%NaCl solution and Hanks solution is about 0.6 V, while the transpassivation stage shifts to the left in sodium citrate solution, and the transpassivation potential drops to about 0.45 V. The lower transpassivation potential indicates that the corrosion resistance of the alloy in sodium citrate solution is poor, and the presence of citrate reduces the corrosion resistance of the alloy. The excellent corrosion resistance of Co-Cr-Mo alloy is due to the spontaneous formation of passivation film; the formation of passivation film will reduce the release of

metal ions, and the destruction of passivation film [20] is the cause of pitting corrosion and gap corrosion. It is believed that the passivation film in the human environment will change with time, and some ions in the electrolyte will be adsorbed to the passivation film and act with some elements to promote the selective dissolution of the passivation film. When the potential reaches a certain value, the Co^{2+} and citrate will be complexed to increase the Co dissolution rate, and the passivation film will be further destroyed, reducing the corrosion resistance of the alloy.

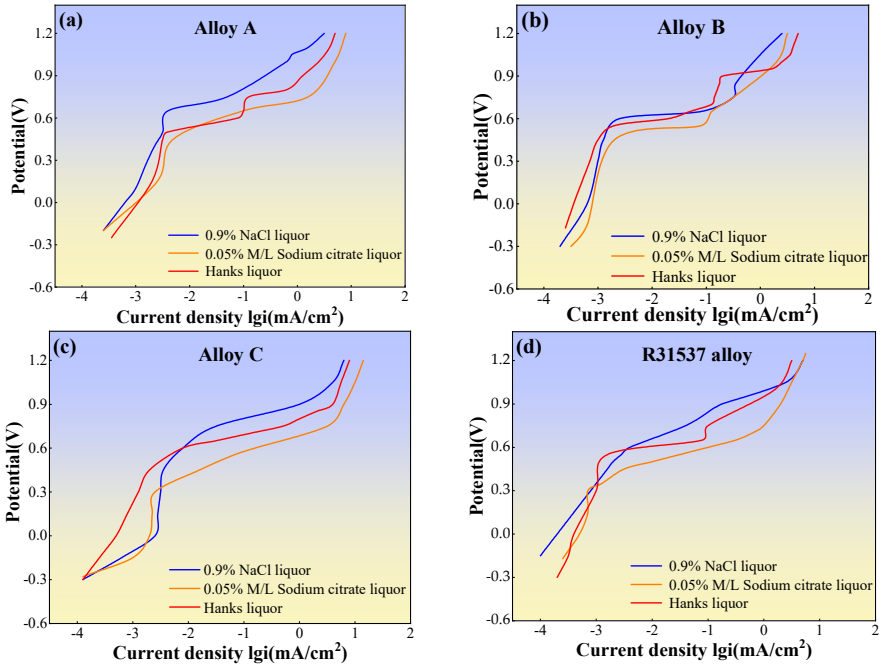

Figure 2. Anodic polarization curves for (**a**) alloy A; (**b**) alloy B; (**c**) alloy C; (**d**) R31537 alloy.

It is found in Figure 2b that B alloy has an obvious passivation process in the three solutions; it not only has a higher passivation potential, but also the passivation zone is wider and more stable, and the secondary passivation occurs when the electrode potential is in the range of 0.7–0.85 V, indicating that B alloy has a better corrosion resistance, which is related to the content of the Cr element in B alloy, and the Cr balance standard potential is much more negative than Fe. Easy to reach a passivation state, under natural conditions or a lot of corrosive media, high corrosion resistance has been shown; not only in oxidizer and oxygen conditions is Cr prone to passivation, even in water, self-passivation can occur, and its passivation state is Cr_2O_3 generated by Cr^{3+} and oxygen reaction, a Cr_2O_3 high melting point, chemical stability and being insoluble in water and acid. Therefore, the higher the content of the Cr element, the more stable passivation film can be generated to protect the alloy from corrosion [21].

Figure 3 shows the fluctuation range of self-corrosion potential Ecorr of three gold combinations in three solutions. The more negative the Ecorr value, the worse the corrosion resistance. It can be seen from Figure 3 that the self-corrosion potential of the four gold combinations is negative, the domestic B alloy self-corrosion potential is relatively higher, and the corrosion resistance is the best, while the foreign R31537 alloy corrosion resistance is the worst, which is closely related [22] to the content of the Cr element in the alloy.

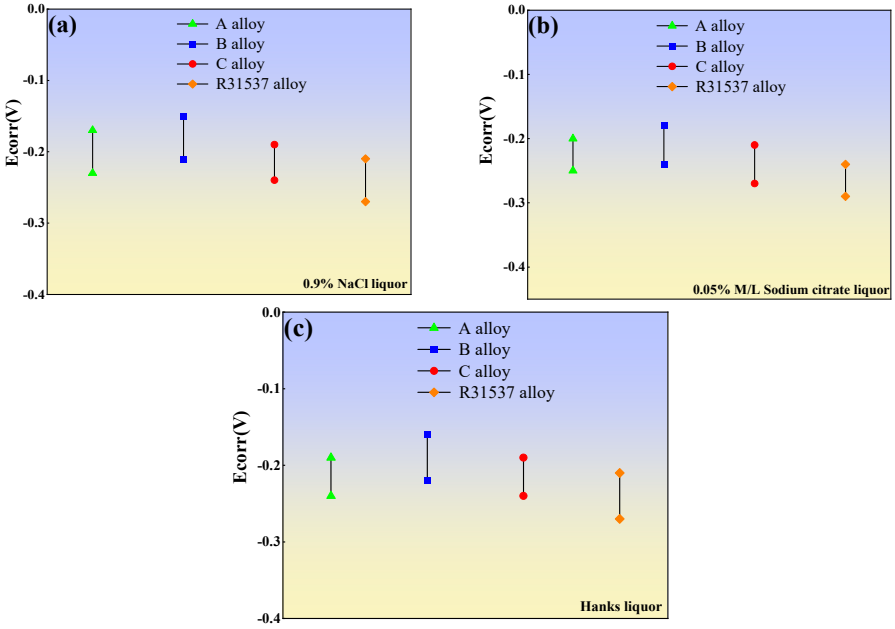

Figure 3. Self-corrosion potential of the four alloys tested in (**a**) 0.9%NaCl solution; (**b**) 0.05%M/L sodium citrate solution; (**c**) Hanks solution.

3.2. Analysis of Biocompatibility of Co-Cr-Mo Alloys in Domestic and Foreign Alloys

3.2.1. Contact Angle

The cells selected in the biocompatibility experiment are mouse osteoblasts, which are adherent-growth cells. In the process of culture, the interaction between cells and the surface of Co-Cr-Mo alloy is firstly adhesion and spreading [23]: the cells are first attached to the surface of the alloy, and then the cell proliferation and differentiation are carried out. Therefore, the hydrophilicity of the Co-Cr-Mo alloy surface has a very important influence [24] on the degree of cell activation and growth state. In this research, the hydrophilicity of Co-Cr-Mo alloy was tested by using a contact Angle measurement experiment with a contact Angle instrument. When the contact Angle is less than 90°, it indicates that Co-Cr-Mo alloy is a hydrophilic material; when the contact Angle is greater than 90°, it indicates that Co-Cr-Mo alloy is a hydrophobic material. The smaller the contact Angle, the more favorable the alloy surface is for cell adhesion and spreading. Figure 4 is the average value calculated after contact Angle measurement at three different locations for four kinds of alloys in domestic and foreign alloys, indicating that Co-Cr-Mo alloy is a hydrophilic material, and foreign R31537 alloy has a smaller contact Angle, and the surface is more suitable for cell adhesion and spreading.

3.2.2. Cytotoxicity

A cytotoxicity experiment is a kind of in vitro experiment simulating the human physiological environment, which is used to detect the biological reaction between medical Co-Cr-Mo alloy and host cells after implantation in the human body, and to evaluate whether toxic reaction occurs between the Co-Cr-Mo alloy and cells after implantation, which is observed under cell microscope after culture for 24 h. By calculating the cell survival rate to evaluate the Co-Cr-Mo alloy by potential cytotoxicity, when the cell survival rate is lower than 70% of the blank control group (control), it indicates that the Co-Cr-Mo alloy has potential cytotoxicity; or the cytotoxicity of Co-Cr-Mo alloy can be evaluated by observing the size of the reaction area under the cell microscope [25]. Figures 5–8 show the growth state of the four alloys in domestic and foreign alloys and the blank control group after 24 h culture. A small number of necrosis and apoptosis cells can be seen in all the four combinations of gold in domestic and foreign alloys, but there is no significant difference from the blank control group. The cells in alloy A and B are in a good spreading state,

indicating that the cells grow well during the culture process, and some cells proliferated. In the domestic C alloy, some of the cells contracted and became small to spheroid, floating in the culture medium, indicating that the cells had died and had no proliferation ability. Most of the cells in foreign R31537 alloy grew normally along the wall; the cell outline was clear, generally spindle or polygon, and individual cells grew fine filamentous pseudopodia, indicating that the cell growth of foreign R31537 alloy was in good [26,27] condition. As there are individual apoptotic and necrotic cells below domestic A, B and foreign R31537 alloys, the toxic reaction of C alloy is limited to below the alloy, so through the analysis of domestic A, B and R31537 alloys, the toxic reaction grade is 1 and the C alloy toxic reaction grade is 2.

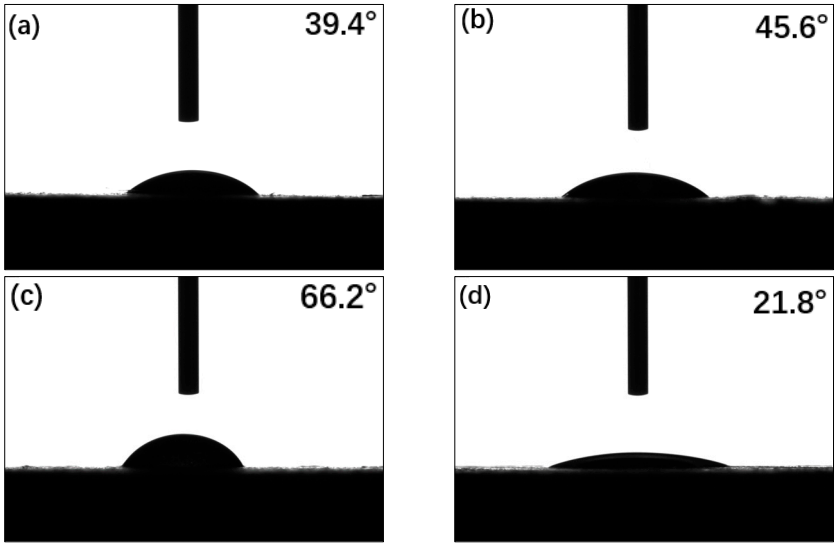

Figure 4. Surface contact angle measurements for (**a**) alloy A; (**b**) alloy B; (**c**) alloy C; (**d**) R31537 alloy.

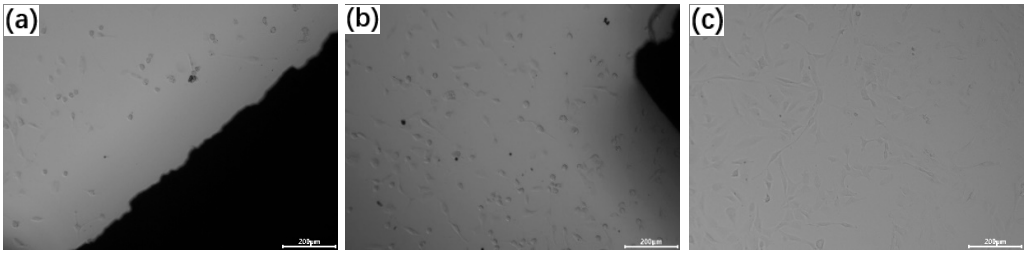

Figure 5. Cell growth after 24 h of domestic alloy A. (**a**) Domestic A alloy. (**b**) Domestic A alloy. (**c**) Control.

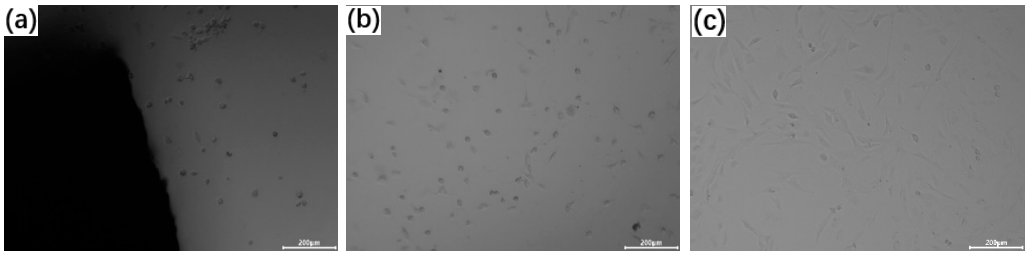

Figure 6. Cell growth after 24 h of domestic alloy B. (**a**) Domestic B alloy. (**b**) Domestic B alloy. (**c**) Control.

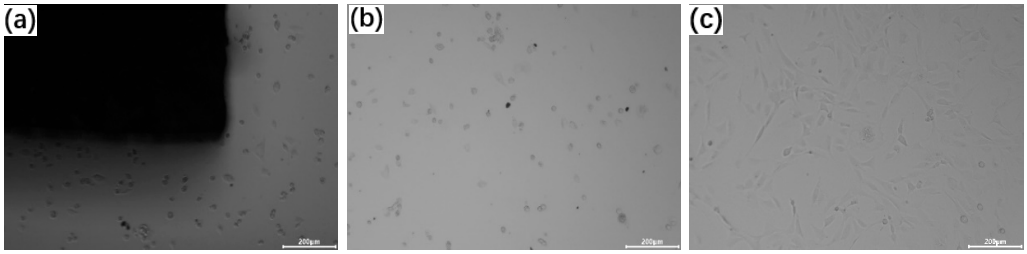

Figure 7. Cell growth after 24 h of domestic alloy C. (**a**) Domestic C alloy. (**b**) Domestic C alloy. (**c**) Control.

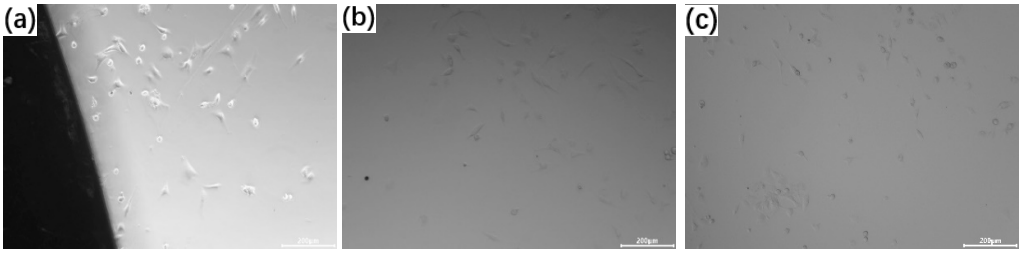

Figure 8. Cell growth after 24 h of foreign alloy C. (**a**) Foreign R31537 alloy. (**b**) Foreign R31537 alloy. (**c**) Control.

Table 5 shows OD values of the four kinds of alloy cells in domestic and foreign alloys. OD values are one of the important indicators to measure cell growth and microbial reproduction. OD values refer to the density of cells in a cell culture medium, that is, the number of cells. OD values are often used to evaluate the growth state of cells in cytotoxicity experiments. In this experiment, the OD value is measured at a specific wavelength and absorbance of the culture medium. Generally speaking, the cell growth rate is proportional to the OD value. The higher the OD value, the higher the cell concentration and the greater the cell number; the growth state [28] of cells can be assessed by the OD value. At the end of the culture, the original medium was sucked, 1 mL of CCK8 working solution (90%MEM + 10%CCK8 detection solution) was added, the hole without cells was used as a blank hole, and after proper incubation time, the hole was properly mixed, and 100 μL of the incubated detection working solution was sucked out from each hole, and the OD value at 450 nm could be measured on the enzyme-labeled instrument. Table 5 shows the OD value of the blank control group and three samples in each group of four gold combinations in domestic and foreign alloys. After calculating the average OD value, it was found that the OD value of the domestic C alloy was relatively low, indicating that the cell concentration of C alloy was low and the number of cells was small, while the OD value of foreign R31537 alloy was the highest, the cell concentration was the highest and the number of cells was the largest. Table 6 is the cell proliferation rate of four kinds of alloys in domestic and foreign alloys; SD in the table represents the standard variance, when evaluating the cell distribution width in the cytotoxicity test; SD is used to reflect the size and dispersion of the cell, generally speaking, the larger the SD value, the more uneven [29] the cell size. According to the formula of cell proliferation rate, the cell proliferation rate of alloy cells in domestic and foreign alloys was calculated by OD value, and the toxic reaction grade of domestic A, B and R31537 alloy was grade 1, and the toxic reaction grade of C alloy was grade 2, which was consistent with the qualitative analysis results.

Sjogren et al. [30] analyzed the influence of alloy composition, pretreatment and operation on alloying element precipitation and found that the change of alloy composition would greatly affect its cytotoxicity. The adverse reactions of some metals and their derivatives to the body have been relatively clear, such as Ni_2S_3, Cr^{6+} and Be derivatives, which are carcinogenic, while some elements are not carcinogenic but can induce mutations and produce adverse biological reactions. Co-Cr-Mo alloy implanted in the human body after service in the human environment, after a long time of friction and wear, is likely to

lead to Co ion dissolution and thus to a cytotoxic reaction; corrosion of the alloy is also extremely important to its biological characteristics, and the type of metal element in the alloy is closely related to its corrosion, in general, the corrosion resistance of precious metals is better than non-precious metals. The dissolution of Co [31,32] ions in Co-Cr-Mo alloy will react with proteins in the human body to form a conjugate, resulting in toxicity, allergy or induced mutation and a series of adverse reactions.

Table 5. Optical density values of the alloys tested in this research.

	OD1	OD2	OD3	OD Average
Blank	0.173	0.171	0.165	0.170
Control	0.933	0.955	0.922	0.937
A alloy	0.752	0.740	0.748	0.747
B alloy	0.793	0.772	0.784	0.783
C alloy	0.676	0.651	0.652	0.670
R31537 alloy	0.823	0.806	0.814	0.814

Table 6. Rate of alloying cell proliferation of the alloys tested in this research.

	Cell Viability (%)			Cell Viability (%) Average	SD
Control	99.52	102.39	98.09	100	2.19
A alloy	76.18	72.58	77.01	75.25	2.35
B alloy	81.58	76.66	81.77	80.00	2.89
C alloy	66.18	61.22	64.33	63.91	2.50
R31537 alloy	85.53	80.99	85.73	84.08	2.68

4. Conclusions

(1) In sodium citrate solution, the transpassivation stage of the four alloys shifted to the left, the potential was about 0.45 V, and the presence of citrate reduced the corrosion resistance of the alloys. All four alloys have a secondary passivation behavior in Hanks solution; when the current is stable, the corrosion rate of the alloy is stable, and the existence of the secondary passivation stage improves the corrosion resistance of the alloy.

(2) Alloy B has an obvious passivation process in the three solutions. It not only has a higher passivation potential, but also the passivation zone is wider and more stable. The secondary passivation occurs when the electrode potential is in the range of 0.7–0.85 V, and the self-corrosion potential of alloy B is relatively higher, indicating that alloy B has better corrosion resistance.

(3) Contact Angle measurement found that the contact Angle of the four alloys in domestic and foreign alloys is less than 90°, indicating that Co-Cr-Mo alloy is a hydrophilic material, foreign R31537 alloy contact Angle is smaller, and the surface is more suitable for cell adhesion and spreading.

(4) The cytotoxicity test found that most of the alloy cells in domestic and foreign alloys showed normal growth along the wall, and the cell outline was clear. For individual cell apoptosis and necrosis, part of the cells under the C alloy contracted and became small to form balls, floating in the culture medium, and the toxicity reaction level of the domestic alloy A, B and R31537 was grade 1, and the toxicity reaction level of the C alloy was grade 2. The C alloy has a slight toxic reaction.

Author Contributions: Conceptualization, B.X. and Y.X.; methodology, B.X.; software, B.X.; validation, B.X., Y.X. and J.W.; formal analysis, B.X.; investigation, B.X.; resources, B.X.; data curation, B.X.; writing—original draft preparation, B.X.; writing—review and editing, B.X.; visualization, B.X.; supervision, B.X.; project administration, B.X.; funding acquisition, Y.X. All authors have read and agreed to the published version of the manuscript.

Funding: This research received no external funding.

Data Availability Statement: The data presented in this study are available on request from the corresponding author.

Conflicts of Interest: The authors declare no conflict of interest.

References

1. Kajima, Y.; Takaichi, A.; Kittikundecha, N.; Nakamoto, T.; Kimura, T.; Nomura, N.; Kawasaki, A.; Hanawa, T.; Takahashi, H.; Wakabayashi, N. Effect of heat-treatment temperature on microstructures and mechanical properties of Co–Cr–Mo alloys fabricated by selective laser melting. *Mater. Sci. Eng. A* **2018**, *726*, 21–31. [CrossRef]
2. Thomann, U.I.; Uggowitzer, P.J. Wear-corrosion behavior of biocompatible austenitic stainless steels. *Wear* **2000**, *239*, 48–58. [CrossRef]
3. Bundy, K.J.; Vogelbaum, M.A.; Desai, V.H. The influence of static stress on the corrosion behavior of 316L stainless steel in Ringer's solution. *J. Biomed. Mater. Res.* **1986**, *20*, 493–505. [CrossRef]
4. Feng, Y.-F.; Kang, H.-F.; Zhang, Z. Study and application of titanium alloy for medical implants. *Rare Met.* **2001**, *25*, 349–354.
5. Reclaru, L.; Lüthy, H.; Eschler, P.Y.; Blatter, A.; Susz, C. Corrosion behavior of cobalt-chromium dental alloys doped with precious metals. *Biomaterials* **2005**, *26*, 4358–4365. [CrossRef]
6. Costello, A.; Sears, J. Repair opportunities for aerospace components through laser powder deposition. In Proceedings of the 25th International Congress on Laser Materials Processing and Laser Microfabrication, Scottsdale, AZ, USA, 30 October–2 November 2006; p. 305.
7. Yingfei, G.; de Escalona, P.M.; Galloway, A. Influence of Cutting Parameters and Tool Wear on the Surface Integrity of Cobalt-Based Stellite 6 Alloy When Machined Under a Dry Cutting Environment. *J. Mater. Eng. Perform.* **2017**, *26*, 312–326. [CrossRef]
8. Mostafaei, A.; Stevens, E.L.; Ference, J.J.; Schmidt, D.E.; Chmielus, M. Binder jetting of a complex-shaped metal partial denture framework. *Addit. Manuf.* **2018**, *21*, 63–68. [CrossRef]
9. Xia, Y.; Zhao, J.; Dong, Z.; Guo, X.; Tian, Q.; Liu, Y. A novel method for making Co-Cr-Mo Alloy spherical powder by granulation and sintering. *JOM* **2020**, *72*, 1279–1285. [CrossRef]
10. Opris, C.D.; Liu, R.; Yao, M.X.; Wu, X.J. Development of stellite alloy composites with sintering/HIPing technique for wear-resistant applications. *Mater. Des.* **2007**, *28*, 581–591. [CrossRef]
11. Sears, J.W.; Allen, C.; Holliday, A. Binder-Jet 3D Direct Metal Printing of Cobalt Chrome Moly Alloy. In Proceedings of the AMPM 2019 Conference, Phoenix, AZ, USA, 23–26 June 2019; pp. 312–321.
12. Hong, D.; Chou, D.-T.T.; Velikokhatnyi, O.I.; Roy, A.; Lee, B.; Swink, I.; Issaev, I.; Kuhn, H.A.; Kumta, P.N. Binder-jetting 3D printing and alloy development of new biodegradable Fe-Mn-Ca/Mg alloys. *Acta Biomater.* **2016**, *45*, 375–386. [CrossRef]
13. Rosenthal, R.; Cardoso, B.R.; Bott, I.S.; Paranhos, R.P.R.; Carvalho, E.A. Phase characterization in as-cast F-75 Co-Cr-Mo-C alloy. *J. Mater. Sci.* **2010**, *45*, 4021–4028. [CrossRef]
14. Huang, P.; Liu, R.; Wu, X.; Yao, M.X. Effects of molybdenum content and heat treatment on mechanical and tribological properties of a low-carbon stellite® Alloy. *J. Eng. Mater. Technol.* **2007**, *129*, 523–529. [CrossRef]
15. Roudnicka, M.; Bigas, J.; Molnarova, O.; Palousek, D.; Vojtech, D. Different response of cast and 3d-printed Co-Cr-Mo alloy to heat treatment: A thorough microstructure characterization. *Metals* **2021**, *11*, 687. [CrossRef]
16. Gui, W.; Long, H.Z.H.; Jin, T.; Qi, X.S. Formation Mechanism of Lamellar $M_{23}C_6$ Carbide in a Cobalt-Base Superalloy During Thermal Exposure at 1000 °C. *Acta Metall. Sin. (Engl. Lett.)* **2018**, *31*, 27–32. [CrossRef]
17. Herranz, G.; Berges, C.; Naranjo, J.A.; García, C.; Garrido, I. Mechanical performance, corrosion and tribological evaluation of a Co–Cr–Mo alloy processed by MIM for biomedical applications. *J. Mech. Behav. Biomed. Mater.* **2020**, *105*, 103706. [CrossRef]
18. Mostafaei, A.; Neelapu, S.H.V.R.; Kisailus, C.; Nath, L.M.; Jacobs, T.D.B.B.; Chmielus, M. Characterizing surface finish and fatigue behavior in binder-jet 3D-printed nickel-based superalloy 625. *Addit. Manuf.* **2018**, *24*, 200–209. [CrossRef]
19. Liao, Y.; Pourzal, R.; Stemmer, P.; Wimmer, M.A.; Jacobs, J.J.; Fischer, A.; Marks, L.D. New insights into hard phases of Co-Cr-Mo metal-on-metal hip replacements. *J. Mech. Behav. Biomed. Mater.* **2012**, *12*, 39–49. [CrossRef]
20. Li, Y.; He, L.; Li, J.; He, J.; Zhuang, Z.; Zhao, J. The content of tumor necrosis factor a in periodontitis gingival tissue and its relationship with periodontitis. *Oral Med.* **2002**, *22*, 12–14.
21. Santos, C.D.; Habibe, A.F.; Simba, B.G.; Lins, J.F.C.; de Freitas, B.X.; Nunes, C.A. Co-Cr-Mo-base alloys for dental applications obtained by selective laser melting (slm) and cad/cam milling. *Mater. Res.* **2020**, *23*, e20190599. [CrossRef]
22. Mori, M.; Yamanaka, K.; Kuramoto, K.; Ohmura, K.; Ashino, T.; Chiba, A. Effect of carbon on the microstructure, mechanical properties and metal ion release of Ni-free Co-Cr-Mo alloys containing nitrogen. *Mater. Sci. Eng. C* **2015**, *55*, 145–154. [CrossRef]
23. Yamanaka, K.; Mori, M.; Chiba, A. Enhanced Mechanical Properties of As-Forged Co-Cr-Mo-N Alloys with Ultrafine-Grained Structures. *Metall. Mater. Trans. A* **2012**, *43*, 5243–5257. [CrossRef]
24. Hasan, S.; Mazid, A.; Clegg, R.E. The Basics of Stellites in Machining Perspective. *Int. J. Eng. Mater. Manuf.* **2016**, *1*, 35–50. [CrossRef]
25. Koju, N.; Niraula, S.; Fotovvati, B. Additively Manufactured Porous Ti-6Al-4V for Bone Implants: A review. *Metals* **2022**, *12*, 687. [CrossRef]
26. Kummrow, A.; Frankowski, M.; Bock, N.; Werner, C.; Dziekan, T.; Neukammer, J. Quantitative assessment of cell viability based on flow cytometry and microscopy. *Cytom. Part A* **2013**, *83*, 197–204. [CrossRef]

27. *ASTM F75-23*; Standard Specification for Cobalt-28 Chromium-6 Molybdenum Alloy Castings and Casting Alloy for Surgical Implants (UNS R30075). ASTM International: West Conshohocken, PA, USA, 2023.
28. Zhu, P.; Chen, J.; Li, P.; Xu, S. Limitation of water-soluble tetrazolium salt for the cytocompatibility evaluation of zinc-based metals. *Materials* **2021**, *14*, 6247. [CrossRef]
29. Wang, Z.; Tang, S.Y.; Scudino, S.; Ivanov, Y.P.; Qu, R.T.; Wang, D.; Yang, C.; Zhang, W.W.; Greer, A.L.; Eckert, J.; et al. Additive manufacturing of a martensitic Co-Cr-Mo alloy: Towards circumventing the strength–ductility trade-off. *Addit. Manuf.* **2021**, *37*, 101725. [CrossRef]
30. Xavier, B.; Freitas, D.; Angelo, C. Sintering behaviour of Co-28%Cr-6%Mo compacted blocks for dental prosthesis. *Integr. Med. Res.* **2019**, *8*, 2052–2062.
31. Dourandish, M.; Godlinski, D.; Simchi, A.; Firouzdor, V. Sintering of biocompatible P/M Co–Cr–Mo alloy (F-75) for fabrication of porosity-graded composite structures. *Mater. Sci. Eng. A* **2008**, *472*, 338–346. [CrossRef]
32. Ziębowicz, A.; Matus, K.; Pawlyta, M.; Pakieła, W.; Matula, G. Comparison of the crystal structure and wear resistance of co-based alloys with low carbon content manufactured by selective laser sintering and powder injection molding. *Crystals* **2020**, *10*, 197. [CrossRef]